Title
Striatal networks for tinnitus treatment targeting.

Journal
Human brain mapping, 43(2)

ISSN
1065-9471

Authors
Hinkley, Leighton BN
Larson, Paul S
Henderson Sabes, Jennifer
et al.

Publication Date
2022-02-01

DOI
10.1002/hbm.25676

Peer reviewed

Received: 14 April 2021 | Revised: 21 September 2021 | Accepted: 21 September 2021

DOI: 10.1002/hbm.25676

RESEARCH ARTICLE

WILEY

Striatal networks for tinnitus treatment targeting

Leighton B. N. Hinkley[1] | Paul S. Larson[2] | Jennifer Henderson Sabes[3] | Danielle Mizuiri[1] | Carly Demopoulos[1,4] | Meredith E. Adams[5] | Thomas C. Neylan[4] | Christopher P. Hess[1] | Srikantan S. Nagarajan[1,3] | Steven W. Cheung[3]

[1]Department of Radiology and Biomedical Imaging, University of California, San Francisco, California

[2]Department of Neurological Surgery, University of California, San Francisco, California

[3]Department of Otolaryngology – Head and Neck Surgery, University of California, San Francisco, California

[4]Department of Psychiatry and Behavioral Sciences, University of California, San Francisco, California

[5]Department of Otolaryngology – Head and Neck Surgery, University of Minnesota Medical School, Minneapolis, Minnesota

Correspondence
Steven W. Cheung, Division of Otology, Neurotology, and Skull Base Surgery, University of California, San Francisco, 2233 Post Street, 3rd Floor, San Francisco, CA 94115.
Email: steven.cheung@ucsf.edu

Funding information
Department of Defense, Grant/Award Numbers: W81XWH-13-1-0494, W81XWH-18-1-0741; National Institute on Deafness and Other Communication Disorders, Grant/Award Number: U01DC013029; U.S. Food and Drug Administration, Grant/Award Number: IDE G120132

Abstract

Neuromodulation treatment effect size for bothersome tinnitus may be larger and more predictable by adopting a target selection approach guided by personalized striatal networks or functional connectivity maps. Several corticostriatal mechanisms are likely to play a role in tinnitus, including the dorsal/ventral striatum and the putamen. We examined whether significant tinnitus treatment response by deep brain stimulation (DBS) of the caudate nucleus may be related to striatal network increased functional connectivity with tinnitus networks that involve the auditory cortex or ventral cerebellum. The first study was a cross-sectional 2-by-2 factorial design (tinnitus, no tinnitus; hearing loss, normal hearing, $n = 68$) to define cohort level abnormal functional connectivity maps using high-field 7.0 T resting-state fMRI. The second study was a pilot case–control series ($n = 2$) to examine whether tinnitus modulation response to caudate tail subdivision stimulation would be contingent on individual level striatal connectivity map relationships with tinnitus networks. Resting-state fMRI identified five caudate subdivisions with abnormal cohort level functional connectivity maps. Of those, two connectivity maps exhibited increased connectivity with tinnitus networks—dorsal caudate head with Heschl's gyrus and caudate tail with the ventral cerebellum. DBS of the caudate tail in the case-series responder resulted in dramatic reductions in tinnitus severity and loudness, in contrast to the nonresponder who showed no tinnitus modulation. The individual level connectivity map of the responder was in alignment with the cohort expectation connectivity map, where the caudate tail exhibited increased connectivity with tinnitus networks, whereas the nonresponder individual level connectivity map did not.

KEYWORDS
caudate nucleus, hearing loss, neuromodulation, striatal networks, tinnitus

Abbreviations: CBda, dorsal anterior caudate body; CBdl, dorsal lateral caudate body; CBdm, dorsal medial caudate body; CBv, ventral caudate body; CHa, anterior caudate head; CHd, dorsal caudate head; CHp, posterior caudate head; CHv, ventral caudate head; CON, normal hearing controls; CT, caudate tail; dB, decibel; DBS, deep brain stimulation; fMRI, functional magnetic resonance imaging; HL, hearing loss without tinnitus; MoCA, montreal cognitive assessment; PTA, pure tone average; TFI, tinnitus functional index; TIN, tinnitus without hearing loss; TIN + HL, tinnitus with hearing loss.

1 | INTRODUCTION

Subjective tinnitus is an auditory phantom disorder characterized by the perception of internally generated elemental sounds, such as ringing, humming, buzzing, chirping, or clicking, in the absence of externally identifiable sources. Its prevalence is 10–15% (Henry, Dennis, & Schechter, 2005; Hoffman & Reed, 2004) and incidence is 5.4% (Martinez, Wallenhorst, McFerran, & Hall, 2015) of the general population. Between 0.5 and 2% of the adult population in the United States are tinnitus sufferers (McFadden, 1982; Vio & Holme, 2005), where auditory phantoms may interfere with activities of daily living, impair mental concentration, disrupt sleep, erode control over auditory phantom percepts, and have relationships with stress, mood, sleep (e.g., insomnia), and compulsive disorders (Betz, Muhlberger, Langguth, & Schecklmann, 2017; Bhatt, Bhattacharyya, & Lin, 2017; Canlon, Theorell, & Hasson, 2013; Cronlein et al., 2016; Hallam, 1996; Henry et al., 2005; Kehrle, Sampaio, Granjeiro, de Oliveira, & Oliveira, 2016; Trevis, McLachlan, & Wilson, 2016; Vanneste et al., 2010). Those relationships, while still poorly defined, may share common neural origins. Over 1 million will remain unresponsive or inadequately responsive to acoustical, behavioral, combined acoustical and behavioral, pharmacological, acupuncture, and other treatments (De Ridder, Joos, & Vanneste, 2016; Dobie, 1999; McFadden, 1982; Vio & Holme, 2005). Without meaningful relief, distressed tinnitus sufferers have participated in invasive experimental brain stimulation procedures (De Ridder, Joos, & Vanneste, 2016; De Ridder, Vanneste, Plazier, et al., 2012; Rammo, Ali, Pabaney, Seidman, & Schwalb, 2018; Tyler et al., 2017), including implantation of deep brain stimulation (DBS) leads into the caudate nucleus of the basal ganglia (Cheung et al., 2019).

Hearing loss is commonly associated with tinnitus (Axelsson & Ringdahl, 1998), and the interaction between hearing loss and tinnitus can compound auditory disabilities (Chung, Gannon, & Mason, 1984; Sindhusake et al., 2004). While sensory end organ damage may be the triggering or key comorbid condition in many cases of acute tinnitus, it is widely accepted that changes in the brain following partial or complete peripheral auditory deafferentation give rise to the neurophysiological bases of chronic tinnitus and treatments for this neuropsychiatric disorder should be directed at the brain (Henry, Roberts, Caspary, Theodoroff, & Salvi, 2014). The examination of central networks for tinnitus have identified several distinct networks that encompass cortical auditory (Norena, 2015; Roberts, 2018; Syka, 2002; Wienbruch, Paul, Weisz, Elbert, & Roberts, 2006) and nonauditory regions (Cheng et al., 2020; De Ridder, Elgoyhen, Romo, & Langguth, 2011; Plewnia et al., 2007; Schlee et al., 2009; Shahsavarani, Schmidt, Khan, Tai, Husain, 2021; Weisz, Moratti, Meinzer, Dohrmann, & Elbert, 2005), and subcortical areas (Cheung & Larson, 2010; Henderson-Sabes et al., 2019; Leaver et al., 2011, 2012; Rauschecker et al., 2010). Tinnitus neuroimaging studies using resting-state fMRI in cohorts with varying levels of hearing loss (Leaver et al., 2011) and stereotyped unilateral profound hearing loss (Henderson-Sabes et al., 2019) have implicated abnormal auditory corticostriatal connectivity as a distinguishing feature. More broadly, several structures within the basal ganglia, including the dorsal/ventral striatum and putamen, have been identified in playing a functional role in tinnitus (Leaver, Seydell-Greenwald, Morgan, Kim, & Rauschecker, 2012; Rauschecker et al., 2010), contributing to potential treatment targets for clinical outcome evaluations. The ventral striatum and ventromedial prefrontal limbic network (Leaver et al., 2012, 2016) has been proposed as a gating mechanism for perceptual phenomena such as tinnitus and chronic pain. This and other limbic networks may be targeted for neuromodulation to mitigate symptom severity. The dorsal striatum has been the only structure where the effects of direct stimulation on tinnitus clinical outcome have been assessed. Acute caudate stimulation in awake and interactive patients undergoing DBS surgery for movement disorders modulated tinnitus percepts in several ways: decreased and increased loudness (Cheung & Larson, 2010), and altered existing auditory phantom sound quality and triggered new auditory phantoms (Larson & Cheung, 2012). Acute caudate stimulation in a phase I clinical trial of DBS for medically refractory tinnitus replicated previously reported stimulation effects (Perez et al., 2019). Chronic caudate stimulation conferred clinically significant benefit to the majority of participants, but with large variations in treatment effect size (Cheung et al., 2019).

The caudate nucleus is a relatively large, inhomogeneous subcortical structure with subdivisions that have been defined neurochemically (Graybiel & Ragsdale Jr, 1978; Holt et al., 1997) and functionally (Jung et al., 2014; Perez et al., 2019). The caudate has distinct patterns of connectivity to brain regions that include auditory (Yeterian & Pandya, 1998), visual (Yeterian & Pandya, 1995), parietal (Yetrerian & Pandya, 1993), and prefrontal (Eblen & Graybiel, 1995; Yeterian & Pandya, 1991) cortices and the thalamus (Ragsdale Jr & Graybiel, 1991). Caudate subdivision heterogeneity may pose treatment targeting challenges for neuromodulation by DBS and other modalities. Moreover, caudate subdivision variations at the single subject, individual level add to the complexity of optimal treatment target selection to maximize tinnitus modulation benefit.

In this study, we addressed treatment target selection for striatal neuromodulation by performing two complementary studies focused on striatal abnormal functional connectivity with tinnitus networks that involve the auditory cortex (Eggermont, 2008; Henry et al., 2014; Norena, 2015; Roberts, 2018) or the ventral cerebellum (Bauer, Kurt, Sybert, & Brozoski, 2013; Brozoski, Ciobanu, & Bauer, 2007). First, in a cohort study, subdivisions with abnormal connectivity to tinnitus networks were identified using high-field strength 7.0 T resting-state fMRI in a 2-by-2 factorial study design (tinnitus, no tinnitus; hearing loss, normal hearing), where the two cohorts with hearing loss were audiometrically matched. Second, in an intervention responder/nonresponder pilot case–control series study, we controlled for treatment target selection (caudate tail subdivision) for neuromodulation by DBS and examined whether difference in individual striatal connectivity pattern (Cheung et al., 2019) was associated with difference in tinnitus modulation clinical outcome. We predicted that stimulation of a caudate subdivision with increased tinnitus network connectivity

would modulate tinnitus and stimulation of a caudate subdivision without abnormal tinnitus network connectivity would not. We evaluated the premise of using single subject level resting-state fMRI striatal connectivity maps for tinnitus modulation. Should this approach to treatment targeting be ultimately validated in the future, it would have immediate implications for other innovative treatment methods, such as direct caudate neuromodulation using MRI guided focused ultrasound (MRgFUS) and proximal striatal neuromodulation effected by stimulation of functionally connected distal cortical targets using repetitive transcranial magnetic stimulation (rTMS) or transcranial direct current stimulation (tDCS).

2 | MATERIALS AND METHODS

2.1 | Participants

Sixty-eight adult participants with constant subjective tinnitus >1 year in duration contributed to the final, completed 7.0 T resting-state fMRI omnibus data set. Eight additional participants were recruited but excluded from final analyses due to poor data quality or intolerance of high field MR. All participants were recruited from Otolaryngology and Audiology clinics, and affiliated facilities of the University of California San Francisco (UCSF). Demographic, audiometric (pure tone average: low (0.5, 1, and 2 kHz), high (4, 6, and 8 kHz), tinnitus severity (Tinnitus Functional Index; TFI) and Montreal Cognitive Assessment (MoCA) scores were collected (Table 1). The four mutually exclusive cohorts were: (a) normal hearing controls (CON, $n = 13$), (b) hearing loss without tinnitus (HL, $n = 12$), (c) tinnitus without hearing loss (TIN, $n = 15$), and (d) tinnitus with hearing loss (TIN + HL, $n = 28$). Sample sizes were sufficient to detect a main contrast (tinnitus, hearing loss) effect size of 0.92 and interaction contrast (tinnitus × hearing loss) effect size of 1.5, with a power of 0.90. Moderate hearing loss was indistinguishable between HL and TIN + HL cohorts. Cohorts were well matched for demographic variables, including sex and handedness (Fisher's Exact test, $p > .05$) as well as education (1×4 ANOVA, $p > .05$). A main effect of age across the cohorts (1×4 ANOVA, $F = 7.31$, $p < .001$) was driven by higher ages in the HL cohort compared to the CON (Tukey HSD $Q = 6.04$, $p < .001$) and TIN (Tukey HSD $Q = 6.08$, $p < .001$) cohorts. No significant differences in MoCA scores were identified among the four groups (1×4 ANOVA, $p > .05$). Exclusion criteria included nonsubjective tinnitus, hearing loss with >10 dB air-bone gap, and MoCA scores <26. All participants gave verbal and written informed consent following full explanation of study procedures. All procedures were approved by the UCSF Committee on Human Research (IRB 13-10587, 13-11641), and all experiments were conducted in accordance with the Declaration of Helsinki. Additionally, two phase I clinical trial participants who underwent experimental striatal stimulation with implanted DBS leads for medically refractory tinnitus contributed 3.0 T resting-state fMRI data and chronic stimulation endpoint tinnitus modulation outcome data reported elsewhere (Cheung et al., 2019).

TABLE 1 Study participants demographics and audiometric characteristics (7 T)

Characteristic	CON	HL	TIN	TIN + HL
N	13	12	15	28
Age[a]	48.8 (11.1)	65.1 (6.8)	49.3 (9.8)	57.3 (11.2)
Education	16.8 (2.1)	16.9 (2.6)	15.9 (2.1)	16.5 (2.5)
Sex	5F/8M	7F/5M	6F/9M	6F/22M
Handedness	12R/1A	10R/2L	12R/3L	26R/2L
Total TFI score	2.5 (2.7)	2.8 (4.7)	47.2 (17.2)	43.4 (32.0)
Pure tone average (left ear)				
Low frequency PTA (dB)	7.7 (6.3)	24.0 (13.1)	9.7 (4.2)	22.1 (11.3)
High frequency PTA (dB)	15.3 (8.9)	51.4 (10.7)	21.3 (8.9)	50.9 (17.9)
Pure tone average (right ear)				
Low frequency PTA (dB)	6.7 (5.3)	25.8 (14.8)	9.7 (4.6)	22.7 (9.8)
High frequency PTA (dB)	15.2 (9.4)	52.3 (15.7)	20.0 (10.0)	50.7 (13.2)
MoCA	28.3 (1.0)	26.9 (2.2)	27.5 (1.2)	27.4 (1.9)

Note: Significant difference in age among cohorts is driven by higher ages in the HL cohort. Moderate hearing loss is matched in the HL and TIN + HL cohorts. Values in mean (SD) where applicable. Tinnitus duration >1 year in all TIN and TIN + HL study participants.

Abbreviations: A, ambidextrous; CON, normal hearing control; dB, decibel; F, female; HL, hearing loss without tinnitus; L, left; M, male; MoCA, Montreal Cognitive Assessment; R, right; TIN, tinnitus without hearing loss; TIN+HL, tinnitus with hearing loss; TFI, Tinnitus Functional Index; PTA, pure tone average.

[a]Main effect of age (1×4 ANOVA, $F = 7.31$, $p < .001$) driven by higher ages in the HL cohort compared to CON ($Q = 6.04$, $p < .001$) and TIN ($Q = 6.08$, $p < .001$) groups. Moderate hearing loss is matched in the HL and TIN + HL cohorts. Values in mean (*SD*) where applicable. Tinnitus duration >1 year in all TIN and TIN + HL study participants.

2.2 | Study design

Cohort level striatal networks in tinnitus and hearing loss were derived from the four cohort data set. 7.0 T MRI data were acquired on GE scanners (GE Healthcare, Waukesha, WI) at the Surbeck Laboratory at the University of California San Francisco. High-resolution T1-weighted anatomical MRIs were acquired using an inversion recovery spoiled gradient echo (IR-SPGR) sequence (1 mm^2 in-plane, 192 1 mm axial slices, TR = 6 ms, TE = 2 ms, TI = 600 ms). High-resolution spontaneous resting-state (eyes closed) data was also collected (1.8 mm^3 isotropic resolution, 76 slices, TR = 4,000 ms, TE = 17 ms, scan length: 6 m:40 s). In order to improve data co-registration, T1-weighted anatomical MRIs acquired in the same subjects at 3.0 T (IR-SPGR; 0.52 mm^2 in-plane, 162 1 mm axial slices, TR = 7 ms, TE = 2 ms, TI = 900 ms) were also acquired and co-registered to the 7.0 T T1-weighted data using tools in SPM12 (https://www.fil.ion.ucl.ac.uk/spm/software/spm12/).

Anatomical and functional deidentified data were spatially preprocessed (e.g., tissue segmentation, co-registration, spatial smoothing at 8 FWHM, artifact rejection, spatial normalization) using the CONN toolbox (https://www.nitrc.org/projects/conn/). Following preprocessing, temporal regressors (gray/white CSF tissue masks, motion parameters) were used to denoise and normalize BOLD signal data (bandpass filtered 0.0008–0.09 Hz).

Seed locations from previously published data were used to generate bilateral 5 mm-radius spheres within each subdivision in Montreal Neurological Institute (MNI) coordinates. Seeds generated by the MarsBaR Matlab toolbox (http://marsbar.sourceforget.net) were between 16 and 23 voxels (isotropic 3 mm resolution). These spherical seeds provided coverage of the caudate nucleus with minimal (<5 voxel) overlap.

Following data acquisition and preprocessing, the caudate nucleus in each hemisphere was segmented into nine subdivisions based on published coordinate (Jung et al., 2014). The corresponding spherical seed locations were positioned to minimize overlap. Functional connectivity maps for each striatal subdivision were defined for the 7.0 T omnibus data set, reproducing the 3.0 T findings by Jung et al. (2014) (Figure S1). The nine caudate subdivisions were named to describe the location of the seed with respect to major anatomical divisions (head, body, and tail): ventral caudate head (CHv), dorsal caudate head (CHd), posterior caudate head (CHp), anterior caudate head (CHa), ventral caudate body (CBv), dorsal anterior caudate body (CBda), dorsal lateral caudate body (CBdl), dorsal medial caudate body (CBdm), and caudate tail (CT).

Individual level striatal networks were reconstructed in the two participants who completed a phase I clinical trial of caudate nucleus DBS for treatment-resistant tinnitus. Demographic information and tinnitus modulation outcome to chronic caudate stimulation for participants U01-10 and U01-12 have already been published (Cheung et al., 2019). We further categorized those trial participants as either responder or nonresponder, using a poststimulation decrease of the baseline TFI score by 13 points as the cutoff value for clinically significant change in tinnitus mitigation (Meikle, Henry, Griest, et al., 2012). Participants U01-10 and U01-12 were selected based on preimplantation neuroimaging data quality suitable for fMRI analysis and each having at least one of their two implanted DBS leads (one in each hemisphere) positioned in caudate subdivision CT. 3.0 T MRI data were acquired on GE scanners (GE Healthcare, Waukesha, WI) at the University of California San Francisco. T1-weighted (FSPGR, 0.5 mm^2 in-plane, 112 axial slices, TR = 7 ms, TE = 3 ms, TI = 800 ms) and 7–8 min of eyes closed resting-state fMRI data (1.88 mm^2 in-plane, TR = 1,739–2,000 ms) were collected prior to surgical implantation. Thirty-one normal hearing controls without tinnitus were also scanned to build a null distribution for construction of individual level maps. To minimize scanner variability, data acquisition for these controls used the same sequences on the same scanner as the two case–control participants.

MRI data was preprocessed using the CONN toolbox and resting-state functional connectivity for the nine subdivisions of the caudate were generated using the same steps outlined above for the 7.0 T cohort study. Functional connectivity maps generated in CONN for each seed were smoothed (4 mm FWHM) for more robust statistical analysis. Functional connectivity maps were generated from left and right seeds separately as DBS lead locations in participant U01-10 differed by hemisphere. This enabled direct comparisons between individual level functional connectivity maps and the cohort level functional connectivity expectation map, and of tinnitus modulation response to electrical stimulation. We identified DBS lead locations in the two trial participants based on the centroid of the distortion artifact generated by the DBS electrodes in postimplantation T1-weighed images in MNI coordinates. The position of this transformed lead location was attributed to a particular subdivision by calculating the three-dimensional Euclidian distance from the centroid to all subdivisions and identifying the subdivision with the shortest distance to the centroid.

2.3 | Statistical analysis

Cohort level functional connectivity maps or expectations maps were determined using statistical engines in the CONN toolbox. Functional connectivity maps for each seed were entered into a voxelwise 2-by-2 factorial ANCOVA modeled with the presence of tinnitus (TIN + HL, TIN) or hearing loss (TIN + HL, HL) as factors, and age as a covariate (higher age in the HL cohort (Table 1), to evaluate main effects of tinnitus and hearing loss, as well as interactions between them. Cluster-level thresholding was generated using parametric Gaussian Random Field theory (RFT; Worsley et al., 1996), with an a priori threshold of p <.001 and a cluster-level p-value threshold of .05 for a false discovery rate (FDR) correction. Statistical output maps were projected onto cortical and cerebellar renderings in SurfIce (https://www.nitrc.org/projects/surfice/).

Individual level tinnitus functional connectivity maps were reconstructed by defining a normative distribution of caudate nucleus subdivisions functional connectivity maps using a resting-state fMRI

protocol in an adult normal hearing without tinnitus control cohort ($n = 31$; mean age = 47.5; female = 15) for comparisons. In turn, those data were used to generate individual level functional connectivity maps for two DBS participants (responder/nonresponder) using a voxelwise *t*-test for comparisons (Crawford & Howell, 1998). Personalized tinnitus striatal networks were cluster corrected (one-tailed $p < .05$, 500 contiguous voxels) and projected onto cortical and cerebellar renderings in SurfIce. This statistical approach has been previously demonstrated to be superior to other techniques when protecting against Type I errors in case–control studies (Crawford & Garthwaite, 2012) .

3 | RESULTS

3.1 | Striatal networks associated with tinnitus

Five caudate subdivisions (CHd, CT, CHp, CBdl, and CHv) exhibited abnormal functional connectivity maps in cohorts with tinnitus (Figure 1; Table 2). Statistical significance for a main effect of tinnitus was determined by comparison between tinnitus (TIN, TIN + HL) and nontinnitus (HL, CON) cohorts ($p < .001$ RFT, $p < .05$ FDR cluster corrected). Increased connectivity was observed between CHd and left Heschl's Gyrus (HG, pink) and between the CT and the right ventral cerebellum (Cb6, green) in TIN and TIN+HL cohorts (Figure 1). Decreased connectivity was observed between CHp and the thalamus bilaterally (Thal, cyan) and the medial geniculate body (MGB) in TIN and TIN + HL cohorts. Increased connectivity was observed between the CHv and the left posterior cerebellum and the left frontal pole (Cb2, FP, yellow;) in the TIN and TIN + HL cohorts, while decreased connectivity was observed between CHv and the right fusiform gyrus (Fus, yellow; Figure 1) in TIN and TIN + HL cohorts. An interaction effect between tinnitus and hearing loss was identified between the connections of CBdl and the right precentral gyrus (PreCG, red; Figure 1). Here, decreased connectivity was observed between these structures but only in patients with tinnitus where hearing loss was absent (TIN) but preserved in patients with tinnitus and hearing loss (TIN + HL; Figure 1).

3.2 | Striatal networks associated with hearing loss

Two caudate subdivisions (CHv, CHa) exhibited decreased functional connectivity in cohorts with hearing loss (Figure 2; Table 3). Statistical significance for a main effect of hearing loss was determined by comparison between hearing loss (TIN + HL, HL) and nonhearing loss (TIN, CON) cohorts ($p < .001$ RFT, $p < .05$ FDR cluster corrected). Decreased connectivity (Figure 2) was observed between CHv and the right hippocampus (HC, yellow) and between CHa with the posterior cingulate bilaterally (PC, blue). No caudate subdivisions showed increased connectivity patterns in hearing loss.

3.3 | Striatal networks correlated with tinnitus severity

Three caudate subdivisions (CT, CHp, and CHa) exhibited significant ($p < .001$ RFT, $p < .05$ FDR cluster corrected) correlations between functional connectivity strength and tinnitus severity (TFI score) in the tinnitus (TIN and TIN + HL, $n = 43$) cohorts (Figure 3; Table 4). Connectivity strength between CT and orbitofrontal cortex (OFC, green) and CT and the precuneus (Precun, green) were negatively correlated with TFI score. Connectivity strength between CHa and the right lateral occipital cortex (LOC, blue) was also negatively correlated with TFI score. Connectivity strength of CHp had mixed effects, where correlation was negative in CHp with the right cerebellum (Cb, cyan) and positive in CHp with the right supramarginal gyrus (SMG, cyan). Connectivity strength between CT and the left postcentral gyrus (PoCG, green) was positively correlated with TFI score.

3.4 | Personalized striatal networks and tinnitus neuromodulation

Tinnitus treatment response to striatal neuromodulation was contingent on personalized connectivity map alignment with the cohort expectation connectivity map, where the caudate tail exhibited increased connectivity with tinnitus networks. The two participants (U01-10 and U01-12) completed a phase I clinical trial of DBS for medically refractory tinnitus (Cheung et al., 2019) and exhibited clear differential responsiveness to caudate subdivision CT stimulation. Participant U01-10 reported exceptional benefit in tinnitus severity reduction while U01-12 reported no benefit.

During intraoperative acute stimulation, U01-10 reported dramatic tinnitus loudness reduction. The left hemisphere DBS lead was positioned in subdivision CT. Tinnitus loudness on a numeric rating scale (0, no tinnitus; 5, conversation level; 10, jet engine) decreased from baseline 8/10 in both ears during surgery to 1/10 in the right and 5/10 in the left ears during stimulation ramp up from 2 to 10 Volts. Stimulation effects washout was fairly rapid, as loudness returned to baseline at 8/10 bilaterally within 1 hr. The right hemisphere DBS lead was positioned in subdivision CBdm. Tinnitus loudness did not change from baseline as incrementally higher stimulation amplitudes were applied, but there was transient tinnitus sound quality change to a lower pitch in the left ear and perception of a new auditory phantom in the right ear. Following a 24-week period of chronic, continuous left CT and right CBdm stimulation, U01-10 reported TFI score decrease by 70 points and tinnitus loudness decrease to 0.5/10 in the right and 2/10 in the left ears (Cheung et al., 2019).

In contrast, U01-12 reported no self-evident tinnitus neuromodulation to acute and chronic striatal stimulation. The left hemisphere DBS lead was positioned in subdivision CT. Tinnitus loudness at baseline was 7/10 in both ears during surgery. Tinnitus sound quality in the right ear became more difficult to discern with stimulation parameter

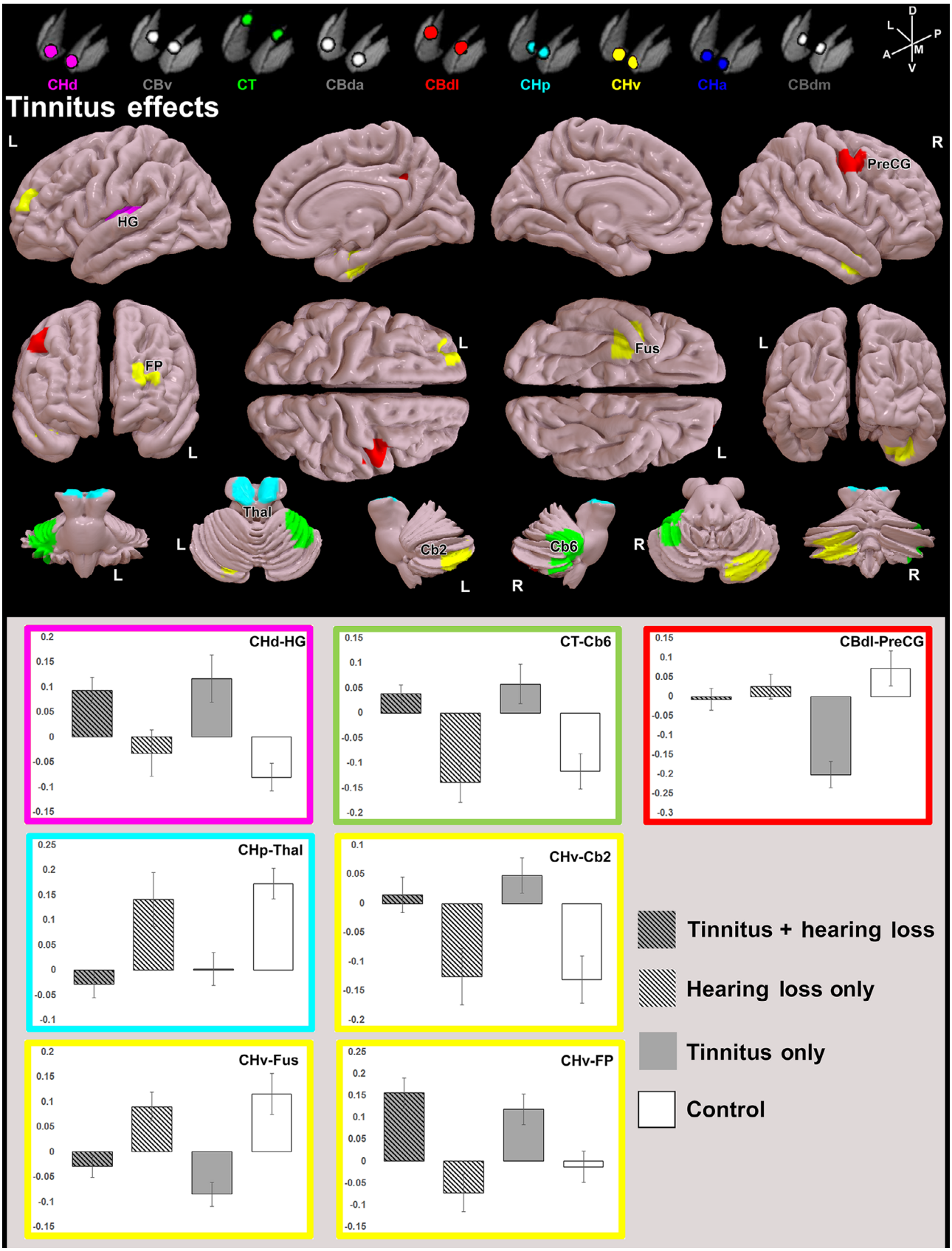

FIGURE 1 Cohort level tinnitus connectivity maps (7 T). Targets that show an effect of tinnitus on functional connectivity are color coded with respect to their corresponding caudate seed: CHd, dorsal caudate head (pink); CT, caudate tail (green); CHp, posterior caudate head (cyan); CBdl, dorsal lateral caudate body (red); CHv, ventral caudate head (yellow). ANCOVA with age as a covariate thresholded at FWE = 0.05. Bounding box color of bar graphs corresponds to caudate seed color. Target cluster descriptions in Table 2. A, anterior; D, dorsal; L, lateral; M, medial; P, posterior; V, ventral

manipulations, but loudness remained unchanged despite variations in stimulation amplitude, frequency, and pulse width. The right hemisphere DBS lead was also positioned in subdivision CT; there was no tinnitus loudness or sound quality neuromodulation. Despite a 24-week period of chronic, continuous left CT and right CT stimulation, U01-12 reported insignificant TFI score decrease by two points and tinnitus loudness increase to 8/10 in both ears.

Personalized striatal networks of tinnitus trial participants U01-10 and U01-12 were markedly different (Figure 4). For U01-10, the left DBS lead positioned in CT corresponded to increased connectivity at this subdivision with the superior parietal lobe (SPL) bilaterally, left temporal lobe along the superior/middle/inferior temporal gyrus, and the left ventral cerebellum (first top row, green box; Figure 4). The right DBS lead positioned in CBdm did not correspond to increased connectivity at this subdivision with either the temporal lobe or cerebellum (second top row, white box; Figure 4). For U01-12, neither the left nor right DBS lead positioned in CT corresponded to increased connectivity with the auditory fields or the cerebellum. U01-12 striatal networks seeded at CT exhibited increased connectivity with frontal regions and the brainstem (third and fourth bottom rows, green box; Figure 4).

4 | DISCUSSION

This is the first study to use high-field resting-state fMRI to delineate tinnitus associated striatal networks of caudate nucleus subdivisions. Subdivisions CHd, CT, CBp, CBdl, and CHv exhibited altered connectivity maps: (a) increased connectivity between CHd and Heschl's gyrus, CT and the ventral cerebellum, and CHv and the posterior cerebellum, and (b) decreased connectivity between CBp and the medial geniculate body, and CBdl and precentral gyrus.

Increased connectivity between the dorsal caudate head (CHd) with primary auditory cortex (HG) using 7.0 T fMRI is an independent replication of the key finding of increased auditory corticostriatal connectivity in chronic tinnitus. Earlier studies acquired data using 3.0 Tesla fMRI in separate cohorts with different hearing loss configurations (Henderson-Sabes et al., 2019; Hinkley, Mizuiri, Hong, Nagarajan, & Cheung, 2015). CHd in the current study represents a spatially circumscribed subdivision that is subsumed by area LC, a larger region qualitatively described as between the junction of the head and body of the caudate nucleus (Cheung & Larson, 2010).

Increased connectivity of the CT subdivision with the ventral cerebellum has clinically relevant behavioral correlates. In a psychophysical rat model of chronic tinnitus induced by unilateral noise exposure, the paraflocculus of the ventral cerebellum showed increased activity and its inactivation by surgical ablation eliminated tinnitus (Bauer et al., 2013; Brozoski et al., 2007). The rat paraflocculus roughly corresponds to the human Cb6 region. Increased connectivity between CT and Cb6, and linear correlation between tinnitus severity and the connectivity strength between CT and OFC, Precun, and PoCG (Figure 3) brings attention to this striatal subdivision as a candidate neuromodulation target and is relevant to our responder-nonresponder analysis below.

Decreased connectivity between the ventral caudate body (CBv) and the MGB of the thalamus is intriguing. While the thalamus is thought to be a factor in tinnitus perception, its exact role is not clear (Caspary & Llano, 2017). One theory, the thalamocortical dysrhythmia hypothesis (De Ridder, Vanneste, Langguth, & Llinas, 2015) posits that phantom auditory percepts are related to asynchronous thalamocortical oscillations, in association with abnormal bursting activity in auditory cortex. Resting-state fMRI studies have reported decreased connectivity between the thalamus and auditory (STG, MTG) and limbic (amygdala) regions (Zhang, Chen, et al., 2015). Our findings of decreased connectivity between subdivision CBv and MGB may reflect a striatal node within an expansive thalamocortical dysrhythmia network.

The solitary identifiable interaction between hearing loss and tinnitus in our dataset—decreased connectivity between subdivision CBdl and the sensorimotor strip (PreCG) in the tinnitus only cohort—highlights the role of the somatosensory system in chronic tinnitus. "Somatosensory tinnitus" is a subtype that may be more common in younger patients and those with normal hearing (Ralli et al., 2016). Interestingly, increased connectivity of the PoCG with caudate subdivision CT was associated with tinnitus severity, implying a more complex role for somatosensory system modulation of striatal networks in tinnitus.

TABLE 2 Tinnitus effects: seeds and target clusters

Seed	Target	Direction	*x*	*y*	*z*	Size	*p* value
Caudate head—dorsal (CHd)	Left Heschl's gyrus (HG)	+	−38	−24	2	107	.014
Caudate tail (CT)	Right Cerebellum-6 (Cb6)	+	30	46	−32	163	<.001
Caudate head—posterior (CHp)	Bilateral thalamus (Thal)	−	−6	−14	6	131	.004
Caudate head—ventral (CHv)	Left cerebellum Crus2 (Cb2)	+	−30	−70	−42	99	.015
	Right temporal fusiform cortex, posterior (Fus)	−	36	−10	−34	96	.018
	Left frontal pole (FP)	+	−28	58	20	64	.109
Caudate body—dorsolateral (CBdl)	Right precentral gyrus (PreCG)[a]	−	48	0	50	83	.037

Note: Brain regions in Figure 1 where statistically significant differences in functional connectivity (7 T) are tabulated with respect to seed, target cluster, connectivity direction (+, increase; −, decrease), target location (Montreal Neurological Institute coordinates), cluster size (voxels), and familywise error corrected *p* value.

[a]Interaction effect of tinnitus and hearing loss only in the tinnitus without hearing loss cohort (TIN).

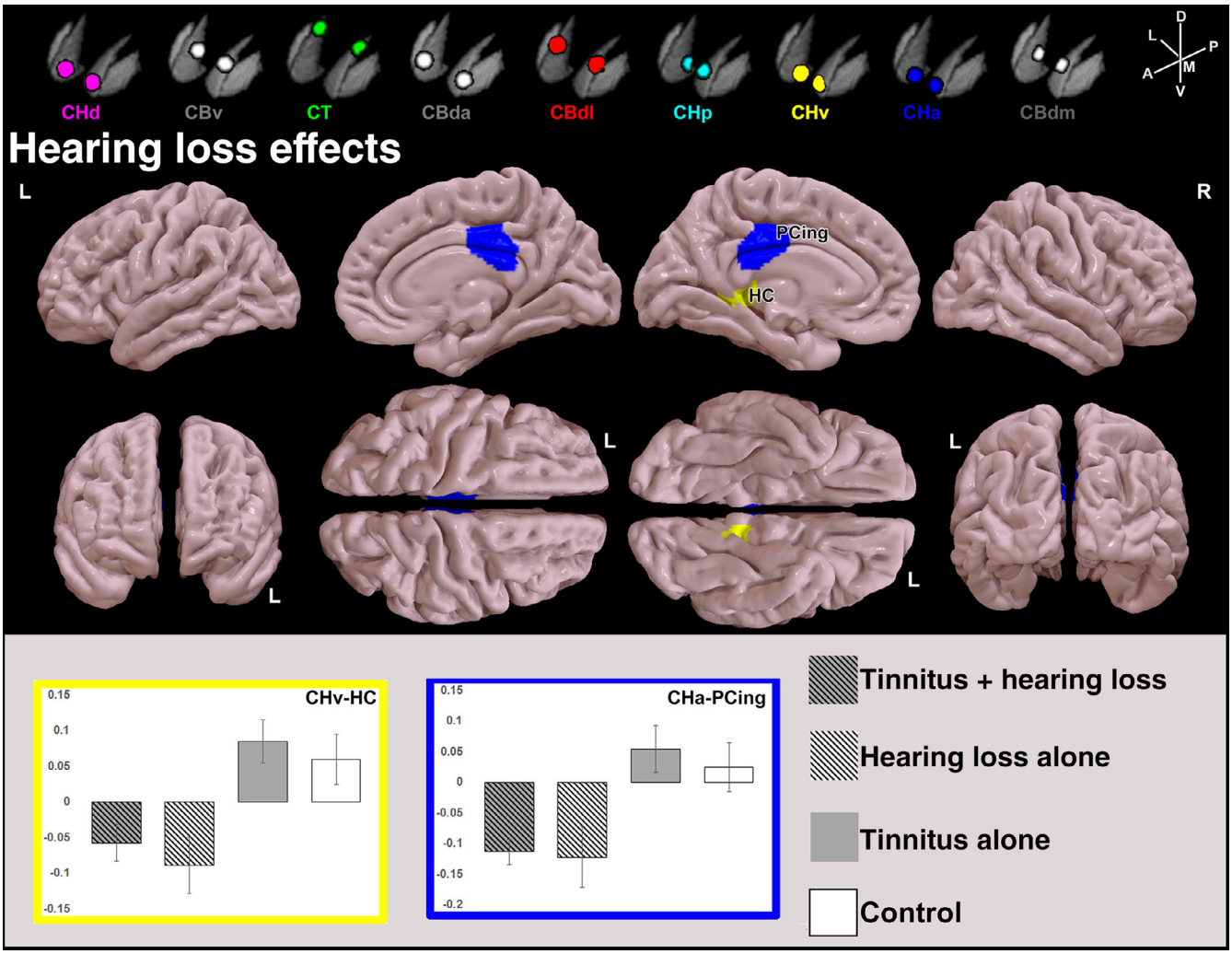

FIGURE 2 Striatal networks associated with hearing loss (7 T). Targets that show an effect of hearing loss on functional connectivity are color coded with respect to their corresponding caudate seed: CHv, ventral caudate head (yellow); CHa, anterior caudate head (blue). Target cluster descriptions in Table 3. Conventions as in Figure 1

TABLE 3 Hearing loss effects: seeds and target clusters

Seed	Target	Direction	*x*	*y*	*z*	Size	*p* value
Caudate head—ventral (CHv)	Left hippocampus (HC)	—	−22	−42	2	108	.009
Caudate head—anterior (CHa)	Cingulate gyrus, posterior (PCing)	—	−2	−22	36	189	<.001

Note: Brain regions in Figure 2 where statistically significant differences in functional connectivity (7 T) are tabulated with respect to seed, target cluster, connectivity direction (+, increase; −, decrease), target location (Montreal Neurological Institute coordinates), cluster size (voxels), and familywise error corrected *p* value.

Linear correlation between tinnitus severity and the connectivity strength between the posterior caudate head (CHp) and the SMG of the temporal lobe suggests neighboring caudate subdivisions may play differential roles in tinnitus perception. Those findings provide further support for the striatal gating hypothesis, where dysfunctional permissiveness of the dorsal striatum gates neural substrates of auditory phantoms into perceptual awareness (Hinkley et al., 2015; Larson & Cheung, 2012).

Striatal functional connectivity alterations due to hearing loss were limited to two caudate subdivisions. CHv and CHa exhibited decreased connectivity with the hippocampus and posterior cingulate, respectively. These findings further support interactions between hearing loss and memory (McCoy et al., 2005; Moon et al., 2020; Rabbitt 1991; Shang et al., 2018; Zhang et al., 2018) and hearing loss and the default mode network (Jung, Colletta, Coalson, Schlaggar, & Lieu, 2017; Zhang, Yang, et al., 2015).

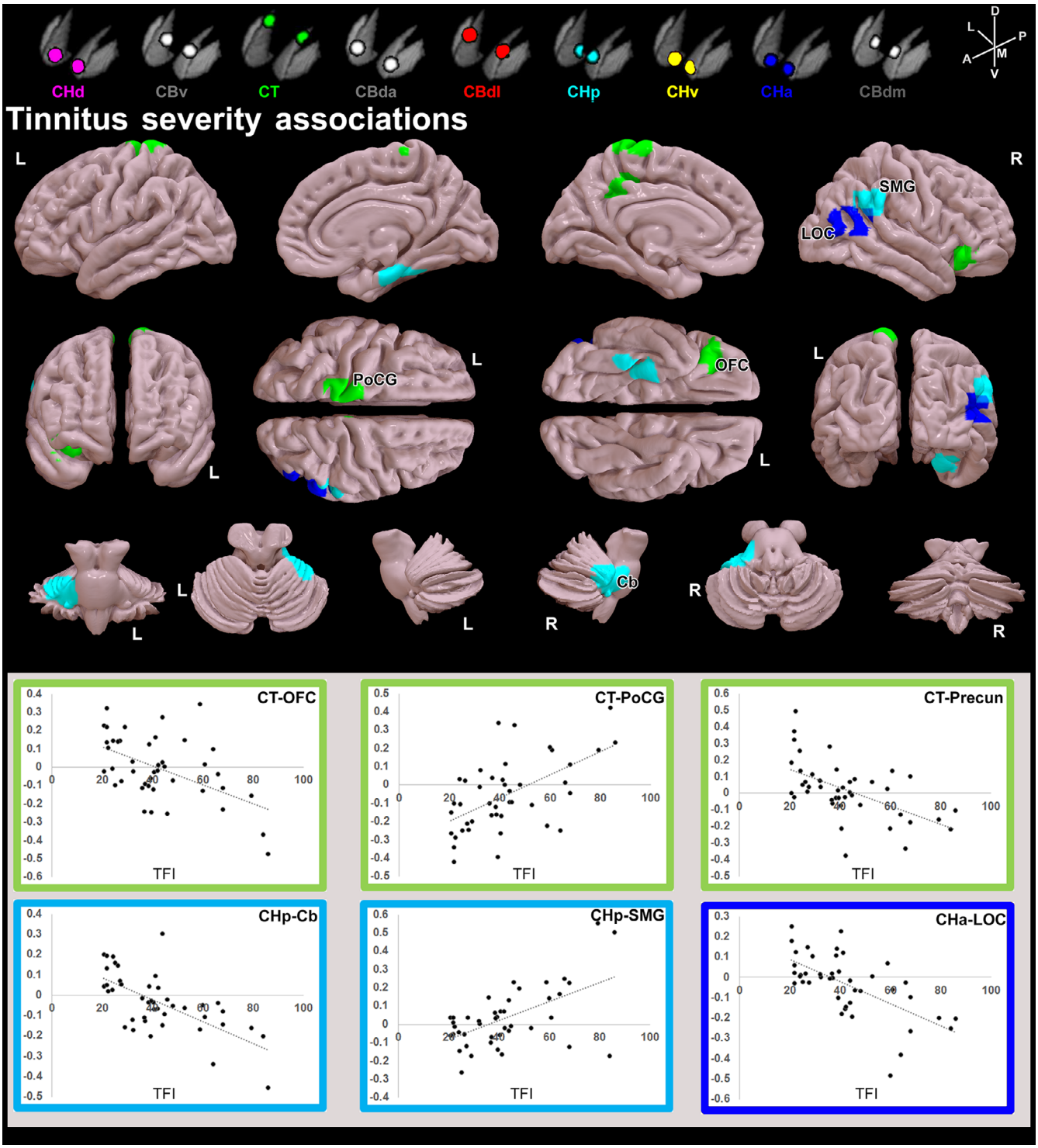

FIGURE 3 Striatal networks associated with tinnitus severity (7 T). Targets that show correlations between functional connectivity strength and tinnitus severity (TFI) are color coded with respect to their corresponding caudate seed: CT, caudate tail (green); CHa, anterior caudate head (in blue); CHp, posterior caudate head (in cyan). Target cluster descriptions in Table 4. Conventions as in Figure 1

Motivated by clear delineations of tinnitus striatal networks at the cohort level, we reconstructed networks at the individual level in two participants who underwent DBS for medically refractory tinnitus. This examination explored translational implications of personalized connectivity maps in neuromodulation target selection. The left DBS lead was positioned in CT in both participants. The right DBS lead was positioned in CBdm in U01-10 and also in CT in U01-12. Subdivision CT striatal networks of responder U01-10 differed from nonresponder U01-12. Increased connectivity between CT and the temporal lobe and the ventral cerebellum was observed only in the

TABLE 4 Regression of connectivity strength and tinnitus severity: seeds and target clusters

Seed	Target	*r*	*x*	*y*	*z*	Size	*p* value
Caudate head—posterior (CHb)	Cerebellum 4,5,6 (Cb456)	−.659	30	−24	−36	140	.002
	Right Supramarginal gyrus, posterior, angular gyrus (SMG/Ang)	.563	66	−44	32	129	.004
Caudate tail (CT)	Precuneus (Precun)	−.568	−14	−42	42	65	.108
	Left postcentral + precentral gyrus (Po/PreCG)	.574	−8	−30	72	94	.021
	Right orbitofrontal cortex (OFC)	−.519	42	30	−12	94	.021
Caudate head—anterior (CHa)	Lateral occipital cortex + angular gyrus (LOC + Ang)	−.638	60	−58	14	254	<.001

Brain regions in Figure 3 with statistically significant linear correlations between functional connectivity strength (7 T) and Tinnitus Functional Index (TFI) score are tabulated with respect to seed, target cluster, correlation (Pearson's *r* value), target location (Montreal Neurological Institute coordinates), cluster size (voxels), and familywise error corrected *p* value.

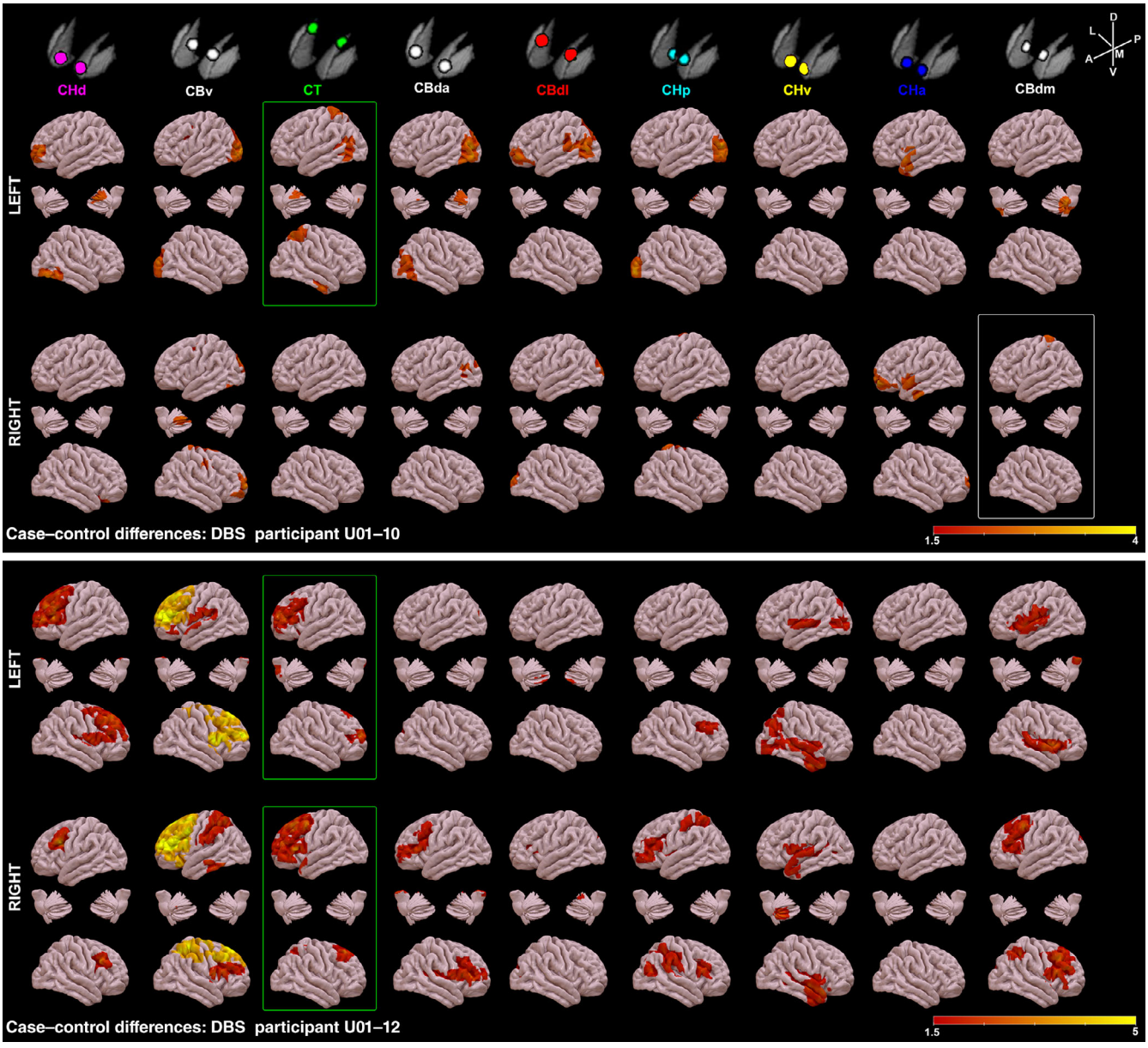

FIGURE 4 Individual level tinnitus connectivity maps (3 T). Caudate neuromodulation responder U01-10 exhibits increased connectivity between left CT and tinnitus networks of cerebellar/temporal regions, in alignment with the cohort level expectation map (Figure 1). Nonresponder U01-12 exhibits increased connectivity between left CT and frontal or brainstem regions bilaterally, without tinnitus network involvement. Rectangular box denotes DBS lead location. Color bar, case–control *t*-statistic; DBS, deep brain stimulation; A, anterior; D, dorsal; L, lateral; M, medial; P, posterior; V, ventral

responder. Furthermore, right CBdm in responder U01-10 did not show increased connectivity with either the temporal lobe or cerebellum, and stimulation of this subdivision yielded subtle tinnitus sound quality modulation without loudness alteration. This provides a within-subject demonstration of individual level striatal map specificity on tinnitus neuromodulation outcomes. Examination of individual variations of striatal network maps highlight how differences can have a profound impact on tinnitus neuromodulation. In this limited responder/nonresponder and within-subject exploration of DBS tinnitus outcomes, personalized striatal network maps appear to be critical for effective treatment target selection.

Beyond DBS, identification of treatment targets for neuromodulation using personalized functional connectivity maps has considerable potential for noninvasive approaches (rTMS/tDCS/MRgFUS). Personalized striatal connectivity maps identify two nodes that may be used to effect neuromodulation: the proximal caudate node, which would require technologies that can stimulate deep brain structures (DBS, MRgFUS), and the distal cortical node, which may be accessed using rTMS and tDCS.

Complementary studies on limbic-auditory interactions suggest that caudate-auditory cortical and caudate-ventral cerebellar networks represent components of a richer set of tinnitus networks. Abnormalities of the ventral striatum, notably the nucleus accumbens, along with its connection to the ventromedial prefrontal cortex (Leaver et al., 2011, 2012; Rauschecker et al., 2010) have been reported in chronic tinnitus. Top-down interactions from these limbic structures with cortical regions are also thought to be dysfunctional in tinnitus (Rauschecker et al., 2010). Additionally, the putamen may also play a role in tinnitus, where aberrant connectivity of this structure with nonauditory networks in tinnitus has been reported (Hinkley et al., 2015; Leaver et al., 2011).

To date, no study has stimulated the aforementioned structures to illuminate the relationships between neuroimaging abnormality and tinnitus modulation. For the ventral striatum and putamen, functional connectivity-based parcellation will be necessary in the future to identify other treatment targets for tinnitus modulation. Such delineation of personalized striatal network maps among tinnitus sufferers may also allow clinicians and investigators to parse heterogeneity in tinnitus perception and responses to conventional acoustical and behavioral therapies. Neuromodulation of multiple tinnitus networks (ventral striatum, dorsal striatum, putamen, etc.) may be required in some treatment-resistant tinnitus patients to deliver meaningful relief.

The consideration for a personalized, patient-specific approach to neuromodulation target selection guided by functional connectivity maps may also be applicable to other brain disorders. Currently, DBS electrode placement is largely dependent on structural MRI for trajectory determination, microelectrode recordings along the path to the target, and electrical stimulation for target confirmation. Despite the good success of DBS for Parkinson's disease (PD), where the treatment targets are relatively small, there is still a need for more tailored approaches (Okun & Foote, 2010). Recent studies support neuroimaging-informed guidance for DBS placement in PD and other disorders, such as depression, obsessive–compulsive disorder, Tourette syndrome, dystonia, and chronic pain (Johnson et al., 2020; Okromelidze et al., 2020; Polanski et al., 2019; Roet et al., 2020; Sullivan, Olsen, & Widge, 2021; Warren et al., 2020) .

Limitations of this study include modest sample sizes for the null distribution derivation that enabled individual level map reconstruction and for the intervention case–control analysis. Future tinnitus neuroimaging studies should expand control data to those without tinnitus across different hearing loss configurations, explicitly match demographic variables, including age, increase data acquisition time for enhancing reliability, and include multiple scanners for data harmonization to assemble a more robust null distribution. Future intervention studies to validate individual level tinnitus network map approach for tinnitus neuromodulation targeting may be performed by interrogating caudate subdivisions directly using incision-free and device-free stimulation technologies, such as magnetic resonance-guided focused ultrasound, and by interrogating associated cortical targets of caudate subdivisions using repetitive transcranial magnetic stimulation.

ACKNOWLEDGMENT

Steven W. Cheung received funding from the Department of Defense (W81XWH-13-1-0494, W81XWH-18-1-0741) and the NIH-NIDCD (U01DC013029) to support this study. Paul S. Larson received an IDE issued by the FDA (IDE no. G120132) to use the Medtronic DBS device for the intervention portion of this study.

CONFLICT OF INTEREST

Paul S. Larson received honoraria from deep brain stimulation (DBS) courses and educational material development for Medtronic, the company that manufactures the DBS device used for the intervention portion of this study.

DATA AVAILABILITY STATEMENT

The datasets generated during and/or analyzed during the current study are available from the corresponding author on reasonable request, subject to University of California applicable data release policies, rules, and regulations.

ORCID

Leighton B. N. Hinkley https://orcid.org/0000-0001-7024-3532
Carly Demopoulos https://orcid.org/0000-0003-2082-3947
Srikantan S. Nagarajan https://orcid.org/0000-0001-7209-3857
Steven W. Cheung https://orcid.org/0000-0003-1724-4944

REFERENCES

Axelsson, A., & Ringdahl, A. (1998). Tinnitus—a study of its prevalence and characteristics. *British Journal of Audiology*, *23*(1), 53–62.

Bauer, C. A., Kurt, W., Sybert, L. T., & Brozoski, T. J. (2013). The cerebellum as a novel tinnitus generator. *Hearing Research*, *295*, 130–139. https://doi.org/10.1016/j.heares.2012.03.009

Betz, L. T., Muhlberger, A., Langguth, B., & Schecklmann, M. (2017). Stress reactivity in chronic tinnitus. *Scientific Reports*, *7*, 41521. https://doi.org/10.1038/srep41521

Bhatt, J. M., Bhattacharyya, N., & Lin, H. W. (2017). Relationships between tinnitus and the prevalence of anxiety and depression. *The Laryngoscope*, *127*(2), 466–469. https://doi.org/10.1002/lary.26107

Brozoski, T. J., Ciobanu, L., & Bauer, C. A. (2007). Central neural activity in rats with tinnitus evaluated with manganese-enhanced magnetic resonance imaging (MEMRI). *Hearing Research*, *228*(1–2), 168–179. https://doi.org/10.1016/j.heares.2007.02.003

Canlon, B., Theorell, T., & Hasson, D. (2013). Associations between stress and hearing problems in humans. *Hearing Research*, *295*, 9–15. https://doi.org/10.1016/j.heares.2012.08.015

Caspary, D. M., & Llano, D. A. (2017). Auditory thalamic circuits and GABA(A) receptor function: Putative mechanisms in tinnitus pathology. *Hearing Research*, *349*, 197–207. https://doi.org/10.1016/j.heares.2016.08.009

Cheng, S., Xu, G., Zhou, J., Qu, Y., Li, Z., He, Z., … Liang, F. (2020). A multimodal meta-analysis of structural and functional changes in the brain of tinnitus. *Frontiers in Human Neuroscience*, *14*, 28. https://doi.org/10.3389/fnhum.2020.00028

Cheung, S. W., & Larson, P. S. (2010). Tinnitus modulation by deep brain stimulation in locus of caudate neurons (area LC). *Neuroscience*, *169*(4), 1768–1778. https://doi.org/10.1016/j.neuroscience.2010.06.007

Cheung, S. W., Racine, C. A., Henderson-Sabes, J., Demopoulos, C., Molinaro, A. M., Heath, S., … Larson, P. S. (2019). Phase I trial of caudate deep brain stimulation for treatment-resistant tinnitus. *Journal of Neurosurgery*, *133*, 992–1001. https://doi.org/10.3171/2019.4.JNS19347

Chung, D. Y., Gannon, R. P., & Mason, K. (1984). Factors affecting the prevalence of tinnitus. *Audiology*, *23*(5), 441–452. https://doi.org/10.3109/00206098409070084

Crawford, J. R., & Garthwaite, P. H. (2012). Single-case research in neuropsychology: A comparison of five forms of t-test for comparing a case to controls. *Cortex*, *48*(8), 1009–1016. https://doi.org/10.1016/j.cortex.2011.06.021

Crawford, J. R., & Howell, D. C. (1998). Comparing an individual's test score against norms derived from small samples. *Clinical Neuropsychology*, *12*(4), 482–486. https://doi.org/10.1076/clin.12.4.482.7241

Cronlein, T., Langguth, B., Pregler, M., Kreuzer, P. M., Wetter, T. C., & Schecklmann, M. (2016). Insomnia in patients with chronic tinnitus: Cognitive and emotional distress as moderator variables. *Journal of Psychosomatic Research*, *83*, 65–68. https://doi.org/10.1016/j.jpsychores.2016.03.001

De Ridder, D., Elgoyhen, A. B., Romo, R., & Langguth, B. (2011). Phantom percepts: Tinnitus and pain as persisting aversive memory networks. *Proceedings of the National Academy of Sciences of the United States of America*, *108*(20), 8075–8080. https://doi.org/10.1073/pnas.1018466108

De Ridder, D., Joos, K., & Vanneste, S. (2016). Anterior cingulate implants for tinnitus: Report of 2 cases. *Journal of Neurosurgery*, *124*(4), 893–901. https://doi.org/10.3171/2015.3.JNS142880

De Ridder, D., Vanneste, S., Langguth, B., & Llinas, R. (2015). Thalamocortical dysrhythmia: A theoretical update in tinnitus. *Frontiers in Neurology*, *6*, 124. https://doi.org/10.3389/fneur.2015.00124

De Ridder, D., Vanneste, S., Plazier, M., Menovsky, T., van de Heyning, P., Kovacs, S., & Sunaert, S. (2012). Dorsolateral prefrontal cortex transcranial magnetic stimulation and electrode implant for intractable tinnitus. *World Neurosurgery*, *77*(5–6), 778–784. https://doi.org/10.1016/j.wneu.2011.09.009

Dobie, R. A. (1999). A review of randomized clinical trials in tinnitus. *The Laryngoscope*, *109*(8), 1202–1211. https://doi.org/10.1097/00005537-199908000-00004

Eblen, F., & Graybiel, A. M. (1995). Highly restricted origin of prefrontal cortical inputs to striosomes in the macaque monkey. *The Journal of Neuroscience*, *15*(9), 5999–6013.

Eggermont, J. J. (2008). Role of auditory cortex in noise- and drug-induced tinnitus. *American Journal of Audiology*, *17*(2), S162–S169.

Graybiel, A. M., & Ragsdale, C. W., Jr. (1978). Histochemically distinct compartments in the striatum of human, monkeys, and cat demonstrated by acetylthiocholinesterase staining. *Proceedings of the National Academy of Sciences of the United States of America*, *75*(11), 5723–5726. https://doi.org/10.1073/pnas.75.11.5723

Hallam, R. S. (1996). Correlates of sleep distubance in chronic distressing tinnitus. *Scandanavian Audiology*, *25*(4), 263–266.

Henderson-Sabes, J., Shang, Y., Perez, P. L., Chang, J. L., Pross, S. E., Findlay, A. M., … Cheung, S. W. (2019). Corticostriatal functional connectivity of bothersome tinnitus in single-sided deafness. *Scientific Reports*, *9*(1), 19552. https://doi.org/10.1038/s41598-019-56127-1

Henry, J. A., Dennis, K. C., & Schechter, M. A. (2005). General review of tinnitus: Prevalence, mechanisms, effects, and management. *Journal of Speech, Language, and Hearing Research*, *48*(5), 1204–1235 Available from http://www.ncbi.nlm.nih.gov/entrez/query.fcgi?cmd=Retrieve&db=PubMed&dopt=Citation&list_uids=16411806

Henry, J. A., Roberts, L. E., Caspary, D. M., Theodoroff, S. M., & Salvi, R. J. (2014). Underlying mechanisms of tinnitus: Review and clinical implications. *Journal of the American Academy of Audiology*, *25*(1), 5–22. https://doi.org/10.3766/jaaa.25.1.2

Hinkley, L. B., Mizuiri, D., Hong, O., Nagarajan, S. S., & Cheung, S. W. (2015). Increased striatal functional connectivity with auditory cortex in tinnitus. *Frontiers in Human Neuroscience*, *9*, 568. https://doi.org/10.3389/fnhum.2015.00568

Hoffman, H. J., & Reed, G. W. (2004). Epidemiology of tinnitus. In J. B. Snow (Ed.), *Tinnitus: Theory and management* (pp. 16–41). Hamilton, ON: BC Decker.

Holt, D. J., Graybiel, A. M., & Saper, C. B. (1997). Neurochemical architecture of the human striatum. *The Journal of Comparative Neurology*, *384*(1), 1–25. https://doi.org/10.1002/(sici)1096-9861(19970721)384:1<1::aid-cne1>3.0.co;2-5

Johnson, K. A., Duffley, G., Anderson, D. N., Ostrem, J. L., Welter, M. L., Baldermann, J. C., … Butson, C. R. (2020). Structural connectivity predicts clinical outcomes of deep brain stimulation for Tourette syndrome. *Brain*, *143*, 2607–2623. https://doi.org/10.1093/brain/awaa188

Jung, M. E., Colletta, M., Coalson, B. S., Schlaggar, B. L., & Lieu, J. E. C. (2017). Differences in interregional brain connectivity in children with unilateral hearing loss. *The Laryngoscope*, *127*, 2636–2645. https://doi.org/10.1002/lary.26587

Jung, W. H., Jang, J. H., Park, J. W., Kim, E., Goo, E. H., Im, O. S., & Kwon, J. S. (2014). Unravelling the intrinsic functional organization of the human striatum: A parcellation and connectivity study based on resting-state FMRI. *PLoS One*, *9*(9), e106768. https://doi.org/10.1371/journal.pone.0106768

Kehrle, H. M., Sampaio, A. L., Granjeiro, R. C., de Oliveira, T. S., & Oliveira, C. A. (2016). Tinnitus annoyance in normal-hearing individuals: correlation with depression and anxiety. *The Annals of Otology, Rhinology, and Laryngology*, *125*(3), 185–194. https://doi.org/10.1177/0003489415606445

Larson, P. S., & Cheung, S. W. (2012). Deep brain stimulation in area LC controllably triggers auditory phantom percepts. *Neurosurgery*, *70*(2), 398–405; discussion 405-6. https://doi.org/10.1227/NEU.0b013e3182320ab5

Leaver, A. M., Renier, L., Chevillet, M. A., Morgan, S., Kim, H. J., & Rauschecker, J. P. (2011a). Dysregulation of limbic and auditory networks in tinnitus. *Neuron*, *69*(1), 33–43.

Leaver, A. M., Seydell-Greenwald, T. T. K., Morgan, S., Kim, H. J., & Rauschecker, J. P. (2012). Cortico-limbic morphology separates tinnitus from tinnitus distress. *Frontiers in Systems Neuroscience*, *6*, 1–14. https://doi.org/10.3389/fnsys.2012.00021

Leaver, A. M., Turesky, T. K., Seydell-Greenwald, A., Morgan, S., Kim, H. J., & Rauschcker, J. P. (2016). Intrinsic network activity in tinnitus investigated using functional MRI. *Human Brain Mapping*, *37*(8), 2717–2735.

Martinez, C., Wallenhorst, C., McFerran, D., & Hall, D. A. (2015). Incidence rates of clinically significant tinnitus: 10-year trend from a cohort study in England. *Ear and Hearing*, *36*(3), e69–e75. https://doi.org/10.1097/AUD.0000000000000121

McCoy, S. L., Tun, P. A., Clarke Cox, L., Colangelo, M., Stewart, R. A., & Wingfield, A. (2005). Hearing loss and perceptual effort: Downstream effects on older adults' memory for speech. *Quarterly Journal of Experimental Psychology*, *58*(1), 22–33.

McFadden, D. (1982). *Tinnitus: Facts, theories, and treatments*. Washington, D.C.: National Academy Press.

Meikle, M. B., Henry, J. A., Griest, S. E., Stewart, B. J., Abrams, H. B., McArdle, R., …, Vernon, J. A. (2012). The tinnitus functional index: Development of a new clinical measure for chronic, intrusive tinnitus. *Ear and Hearing*, *33*(2), 153–176. https://doi.org/10.1097/AUD.0b013e31822f67c0

Moon, P. K., Qian, J. Z., McKenna, E., Xi, K., Rowe, N. C., Ng, N. N., … Yeom, K. W. (2020). Cerebral volume and diffusion MRI changes in children with sensorineural hearing loss. *Neuroimage: Clinical*, *27*, 102328. https://doi.org/10.1016/j.nicl.2020.102328

Norena, A. J. (2015). Revisiting the cochlear and central mechanisms of tinnitus and therapeutic approaches. *Audiology & Neuro-Otology*, *20*-(Suppl 1), 53–59. https://doi.org/10.1159/000380749

Okromelidze, L., Tsuboi, T., Eisinger, R. S., Burns, M. R., Charbel, M., Rana, M., … Middlebrooks, E. H. (2020). Functional and structural connectivity patterns associated with clinical outcomes in deep brain stimulation of the Globus Pallidus Internus for generalized dystonia. *American Journal of Neuroradiology*, *41*(3), 508–514. https://doi.org/10.3174/ajnr.A6429

Okun, M. S., & Foote, K. D. (2010). Parkinson's disease DBS: What, when, who and why? The time has come to tailor DBS targets. *Expert Review of Neurotherapeutics*, *10*(12), 1847–1857. https://doi.org/10.1586/Ern.10.156

Perez, P. L., Wang, S. S., Heath, S., Henderson-Sabes, J., Mizuiri, D., Hinkley, L. B., … Cheung, S. W. (2019). Human caudate nucleus subdivisions in tinnitus modulation. *Journal of Neurosurgery*, *132*, 1–7. https://doi.org/10.3171/2018.10.JNS181659

Plewnia, C., Reimold, M., Najib, A., Brehm, B., Reischl, G., Plontke, S. K., & Gerloff, C. (2007). Dose-dependent attenuation of auditory phantom perception (tinnitus) by PET-guided repetitive transcranial magnetic stimulation. *Human Brain Mapping*, *28*(3), 238–246.

Polanski, W. H., Zolal, A., Klein, J., Kitzler, H. H., Schackert, G., Eisner, W., & Sobottka, S. B. (2019). Somatosensory functional MRI tractography for individualized targeting of deep brain stimulation in patients with chronic pain after brachial plexus injury. *Acta Neurochirurgica*, *161*(12), 2485–2490. https://doi.org/10.1007/s00701-019-04065-2

Rabbitt, P. (1991). Mild hearing loss can cause apparent memory failures which increase with age and reduce with IQ. *Acta Otolaryngologica*, *476*, 167–176.

Ragsdale, C. W., Jr., & Graybiel, A. M. (1991). Compartmental organization of the thalamostriatal connection in the cat. *The Journal of Comparative Neurology*, *311*(1), 134–167. https://doi.org/10.1002/cne.903110110

Ralli, M., Altissimi, G., Turchetta, R., Mazzei, F., Salviati, M., Cianfrone, F., … Cianfrone, G. (2016). Somatosensory tinnitus: Correlation between cranio-cervico-mandibular disorder history and somatic modulation. *Audiology and Neurotology*, *21*(6), 372–382. https://doi.org/10.1159/000452472

Rammo, R., Ali, R., Pabaney, A., Seidman, M., & Schwalb, J. (2018). Surgical neuromodulation of tinnitus: A review of current therapies and future applications. *Neuromodulation*, *22*, 380–387. https://doi.org/10.1111/ner.12793

Rauschecker, J. P., Leaver, A. M., & Muhlau, M. (2010a). Tuning out the noise: Limbic-auditory interactions in tinnitus. *Neuron*, *66*(6), 819–826.

Roberts, L. E. (2018). Neural plasticity and its initiating conditions in tinnitus. *HNO*, *66*(3), 172–178. https://doi.org/10.1007/s00106-017-0449-2

Roet, M., Boonstra, J., Sahin, E., Mulders, A. E. P., Leentjens, A. F. G., & Jahanshahi, A. (2020). Deep brain stimulation for treatment-resistant depression: Towards a more personalized treatment approach. *Journal of Clinical Medicine*, *9*(9), 1–20. https://doi.org/10.3390/jcm9092729

Schlee, W., Mueller, N., Hartmann, T., Keil, J., Lorenz, I., & Weisz, N. (2009). Mapping cortical hubs in tinnitus. *BMC Biology*, *7*, 80.

Shahsavarani, S., Schmidt, S. A., Khan, R. A., Tai, Y., & Husain, F. T. (2021). Salience, emotion, and attention: The neural networks underlying tinnitus distress revealed using music and rest. *Brain Research*, *1755*, 147277. https://doi.org/10.1016/j.brainres.2021.147277

Shang, Y., Hinkley, L. B., Cai, C., Subramaniam, K., Chang, Y. S., Owen, J. P., … Cheung, S. W. (2018). Functional and structural brain plasticity in adult onset single-sided deafness. *Frontiers in Human Neuroscience*, *12*, 474. https://doi.org/10.3389/fnhum.2018.00474

Sindhusake, D., Golding, M., Wigney, D., Newall, P., Jakobsen, K., & Mitchell, P. (2004). Factors predicting severity of tinnitus: A population-based assessment. *Journal of the American Academy of Audiology*, *15*(4), 269–280. https://doi.org/10.3766/jaaa.15.4.2

Sullivan, C. R. P., Olsen, S., & Widge, A. S. (2021). Deep brain stimulation for psychiatric disorders: From focal brain targets to cognitive networks. *NeuroImage*, *225*, 117515. https://doi.org/10.1016/j.neuroimage.2020.117515

Syka, J. (2002). Plastic changes in the central auditory system after hearing loss, restoration of function, and during learning. *Physiological Reviews*, *82*(3), 601–636. https://doi.org/10.1152/physrev.00002.2002

Trevis, K. J., McLachlan, N. M., & Wilson, S. J. (2016). Psychological mediators of chronic tinnitus: The critical role of depression. *Journal of Affective Disorders*, *204*, 234–240. https://doi.org/10.1016/j.jad.2016.06.055

Tyler, R., Cacace, A., Stocking, C., Tarver, B., Engineer, N., Martin, J., … Vanneste, S. (2017). Vagus nerve stimulation paired with tones for the treatment of tinnitus: A prospective randomized double-blind controlled pilot study in humans. *Scientific Reports*, *7*(1), 11960. https://doi.org/10.1038/s41598-017-12178-w

Vanneste, S., Plazier, M., der Loo, E., de Heyning, P. V., Congedo, M., & De Ridder, D. (2010). The neural correlates of tinnitus-related distress. *NeuroImage*, *52*(2), 470–480. https://doi.org/10.1016/j.neuroimage.2010.04.029

Vio, M. M., & Holme, R. H. (2005). Hearing loss and tinnitus: 250 million people and a US$10 billion potential market. *Drug Discovery Today*, *10*(19), 1263–1265. http://www.ncbi.nlm.nih.gov/entrez/query.fcgi?cmd=Retrieve&db=PubMed&dopt=Citation&list_uids=16214667

Warren, A. E. L., Dalic, L. J., Thevathasan, W., Roten, A., Bulluss, K. J., & Archer, J. (2020). Targeting the centromedian thalamic nucleus for deep brain stimulation. *Journal of Neurology, Neurosurgery, and Psychiatry*, *91*(4), 339–349. https://doi.org/10.1136/jnnp-2019-322030

Weisz, N., Moratti, S., Meinzer, M., Dohrmann, K., & Elbert, T. (2005). Tinnitus perception and distress is related to abnormal spontaneous brain activity as measured by magnetoencephalography. *PLoS Medicine*, *2*(6), e153.

Wienbruch, C., Paul, I., Weisz, N., Elbert, T., & Roberts, L. E. (2006). Frequency organization of the 40-Hz auditory steady-state response in normal hearing and in tinnitus. *NeuroImage*, *33*(1), 180–194.

Worsley, K. J., Marrett, S., Neelin, P., Vandal, A. C., Friston, K. J., & Evans, A. C. (1996). A unified statistical approach for determining significant signals in images of cerebral activation. *Human Brain Mapping*, *4*(1), 58–73. https://doi.org/10.1002/(SICI)1097-0193(1996)4:1<58::AID-HBM4>3.0.CO;2-O

Yeterian, E. H., & Pandya, D. N. (1991). Prefrontostriatal connections in relation to cortical architectonic organization in rhesus monkeys. *The Journal of Comparative Neurology*, *312*(1), 43–67. https://doi.org/10.1002/cne.903120105

Yeterian, E. H., & Pandya, D. N. (1993). Striatal connections of the parietal association cortices in rhesus monkeys. *The Journal of Comparative Neurology*, *332*(2), 175–197. https://doi.org/10.1002/cne.903320204

Yeterian, E. H., & Pandya, D. N. (1995). Corticostriatal connections of extrastriate visual areas in rhesus monkeys. *The Journal of Comparative Neurology*, *352*(3), 436–457. https://doi.org/10.1002/cne.903520309

Yeterian, E. H., & Pandya, D. N. (1998). Corticostriatal connections of the superior temporal region in rhesus monkeys. *The Journal of Comparative Neurology*, *399*(3), 384–402.

Zhang, G. Y., Yang, M., Liu, B., Huang, Z. C., Chen, H., Zhang, P. P., … Teng, G. J. (2015). Changes in the default mode networks of individuals with long-term unilateral sensorineural hearing loss. *Neuroscience*, *285*, 333–342.

Zhang, J., Chen, Y. C., Feng, X., Yang, M., Liu, B., Qian, C., … Teng, G. J. (2015). Impairments of thalamic resting-state functional connectivity in patients with chronic tinnitus. *European Journal of Radiology*, *84*(7), 1277–1284. https://doi.org/10.1016/j.ejrad.2015.04.006

Zhang, Y., Mao, Z., Feng, S., Liu, X., Lan, L., Zhang, J., & Yu, X. (2018). Altered functional networks in long-term unilateral hearing loss: A connectome analysis. *Brain and Behavior: A Cognitive Neuroscience Perspective*, *8*(2), e00912. https://doi.org/10.1002/brb3.912

SUPPORTING INFORMATION

Additional supporting information may be found in the online version of the article at the publisher's website.

How to cite this article: Hinkley, L. B. N., Larson, P. S., Henderson Sabes, J., Mizuiri, D., Demopoulos, C., Adams, M. E., Neylan, T. C., Hess, C. P., Nagarajan, S. S., & Cheung, S. W. (2022). Striatal networks for tinnitus treatment targeting. *Human Brain Mapping*, *43*(2), 633–646. https://doi.org/10.1002/hbm.25676